

Local Density Fluctuation Governs Divergence of Viscosity underlying Elastic and Hydrodynamic Anomalies in a 2D Glass-Forming Liquid

Hayato Shiba,¹ Takeshi Kawasaki,² and Kang Kim³

¹*Institute for Materials Research, Tohoku University, Sendai 980-8577, Japan*

²*Department of Physics, Nagoya University, Nagoya 464-8602, Japan*

³*Division of Chemical Engineering, Graduate School of Engineering Science, Osaka University, Osaka 560-8531, Japan*

(Dated: December 25, 2019)

If a liquid is cooled rapidly to form a glass, its structural relaxation becomes retarded, producing a drastic increase in viscosity. In two dimensions, strong long-wavelength fluctuations persist, even at low temperature, making it difficult to evaluate the microscopic structural relaxation time. This Letter shows that, in a 2D glass-forming liquid, relative displacement between neighbor particles yields a relaxation time that grows in proportion to the viscosity. In addition to thermal elastic vibrations, hydrodynamic fluctuations are found to affect the long-wavelength dynamics, yielding a logarithmically diverging diffusivity in the long-time limit.

In many two-dimensional ordering phenomena, fluctuations at long wavelengths are so strong that perfect order is destroyed. For example, the transition between a liquid and a crystalline solid is continuous or nearly continuous [1–6]. Recently, large-scale molecular dynamics (MD) simulations [7, 8] and colloidal experiments [9, 10] have revealed that such long-wavelength fluctuations also exist in two-dimensional (2D) liquids that are rapidly cooled toward the glass transition. Although retaining a random amorphous structure, elastic vibrations appear as the rigidity emerges with the decrease in temperature. The excess of low-frequency phonons in two dimensions [7, 11] leads to an elastic anomaly, where the amplitude of thermal vibrations diverge at long wavelengths. Even in the presence of these long-wavelength fluctuations, the microscopic structural relaxations in 2D and 3D supercooled liquids appear to be similar, once the effect of these fluctuations has been eliminated by introducing quantities that characterize the local switching between neighbor particles [7, 9, 10].

Albeit a similarity of structural relaxation modality between 2D and 3D glass-forming liquids, it does not mean that the transport properties, a key to the nature of glass transitions, are similar in between. One problem lies in the relationship between the structural relaxation time and the viscosity. The glass transition is marked by a drastic increase in macroscopic viscosity with decreasing temperature, which is intimately related to the divergence of the microscopic structural relaxation time. As such, theoretical and computational studies have focused on the dynamical mechanism of growth in the microscopic structural relaxation time, most typically the α -relaxation time τ_α [12–15], defined as the decay time of the relaxation function for density fluctuations, *i.e.*, the intermediate scattering function. However, in two dimensions, the strong density fluctuation diverges at long wavelengths and suppresses its intermediate plateau. Thus, τ_α no longer represents the microscopic structural relaxation time. The first problem arises on how to define the relaxation time that represents viscous slowdown of the dynamics.

Furthermore, a more intriguing problem lies in the potential role of hydrodynamic effects on the transport properties.

For a liquid in two dimensions, a slow t^{-1} decay (the so-called long-time tail) of the velocity and stress autocorrelation functions leads to a *hydrodynamic anomaly* that is marked by a logarithmic divergence of transport coefficients such as diffusivity and viscosity [16–19]. How it alters the transport properties of deeply cooled liquids at the macroscopic level is a fully open issue, and the glass transition may be influenced by a mechanism that is different from the freezing of microscopic structural relaxation due to the cage effect. In fact, it is difficult to distinguish the characteristic time scales of the long-time tail and the microscopic structural relaxation, both of which become significantly large upon supercooling. Such long-wavelength fluctuations derived from hydrodynamics may even possibly prohibit the 2D glass transition. Therefore, in addition to the effect of elastic fluctuations that inhibit the existence of 2D crystals, it is important to reveal how macroscopic hydrodynamic fluctuations can influence the microscopic structural relaxation in 2D glass-forming liquids.

In this Letter, in order to address these issues, we perform large-scale MD simulations of a 2D glass-forming liquid to examine how the growth of various relaxation times is related to the divergence of macroscopic viscosity in the presence of long-wavelength fluctuations. The simulations are performed with a particular focus on how the dynamics depend on the system size, so that the anomalous enhancement of elastic and hydrodynamic responses can be characterized. Simulations are performed for a 2D variant of Kob–Andersen binary Lennard–Jones mixtures [20], in which the composition is 65:35 [8, 21–23]. The mixture is annealed for a sufficiently long time (maximum of 4×10^9 simulation steps) after rapid cooling to target temperatures in the range $0.4 \leq T \leq 1.0$ in the presence of Langevin heat baths. The production runs are then performed as Newtonian (*NVE*) dynamics simulations to prevent the damping of long-wavelength fluctuations. The data presented in the remainder of this Letter are averaged over four or eight independent simulations [24].

First, we revisit three relaxation functions that have been considered in recent studies [7–10, 23]. The first is the standard self-intermediate scattering function (SISF) $F_s(k, t) = (1/N) \langle \sum_{j=1}^N \exp[i\mathbf{k} \cdot (\mathbf{r}_j(t + t_0) - \mathbf{r}_j(t_0))] \rangle$, with the wavevec-

tor set to $|\mathbf{k}| = 2\pi/\sigma_{11}$ so that its decay represents particle movement over a distance of the particle diameter σ_{11} . However, in two dimensions, long-wavelength elastic vibrations persist, and these enhance the mean-squared thermal displacement δ^2 [7, 25]. Figure 1 shows the SISF for a fixed temperature $T = 0.4$, where the size-dependent behavior is in agreement with previous studies [7, 8]. The plateau heights represent the Debye–Waller factor $f_p \sim \exp(-k^2\delta^2/2)$ [24, 26], and tend toward zero as the system size increases. Therefore, the α -relaxation time (the decay time of the SISF) is strongly influenced by long-wavelength fluctuations and cannot represent the microscopic structural relaxation time.

The other two functions are the “neighbor-relative” SISF (also known as the “cage-relative” SISF [9, 10, 23, 27, 28]) and bond relaxation function [22, 29–31]. These are also plotted in Fig. 1. The latter two functions represent relaxations in the sense that the long-wavelength thermal vibrations are removed. The former is defined by

$$F_s^R(k, t) = (1/N) \left\langle \sum_{j=1}^N \exp\{i\mathbf{k} \cdot \Delta\mathbf{r}_j^{\text{rel}}(t)\} \right\rangle. \quad (1)$$

We here introduce the *neighbor-relative* displacement $\Delta\mathbf{r}_i^{\text{rel}}(t) = (1/N_{\text{n.n.}}) \sum_{j \in \text{n.n.}} [\Delta\mathbf{r}_i(t) - \Delta\mathbf{r}_j(t)]$ (also known as the “cage-relative” displacement [9, 10, 32]), where the summation is over $N_{\text{n.n.}}$ initially neighboring pairs of particles, indicating the changes in the relative positions. A similar displacement was considered in previous studies on 2D melting for the same purpose of eliminating long-wavelength fluctuations [3, 33, 34]. The bond relaxation function $F_B(t)$, in contrast, does not involve displacements of the particles, but simply characterizes the proportion of initially neighboring pairs that have survived after a certain time [24]. From the observation that neither function is strongly dependent on the system size, contrary to the standard SISF, the effect of long-wavelength fluctuations is marginal for these relaxation functions, as expected from their definitions.

Along with our aim to relate these microscopic relaxation functions with the macroscopic viscosity, Fig. 1 also shows the stress relaxation function (or “dynamic modulus” [23])

$$G(t) = \frac{V}{k_B T} \langle \sigma_{xy}(t) \sigma_{xy}(0) \rangle, \quad (2)$$

where $\sigma_{xy}(t)$ is the off-diagonal stress tensor (the data are normalized with respect to the instantaneous shear modulus $G_\infty = G(0)$). $G(t)$ exhibits a stretched plateau modulus and no system size dependence at a low temperature of $T = 0.4$, as shown in Fig. 1. In a recent paper, the plateau was found to become unclear, rendering it difficult to evaluate the plateau modulus, for higher temperatures at the onset of slow dynamics, $T \geq 0.7$ [23].

Next, we define relaxation times and compare them with the transport coefficients —the α -relaxation time τ_α , neighbor-relative relaxation time τ_R , and bond relaxation time τ_B can be defined as the decay times of the standard SISF, neighbor-relative SISF, and bond relaxation functions [24]. For this purpose, we refer to the Stokes–Einstein (SE) relation $D\eta/T =$

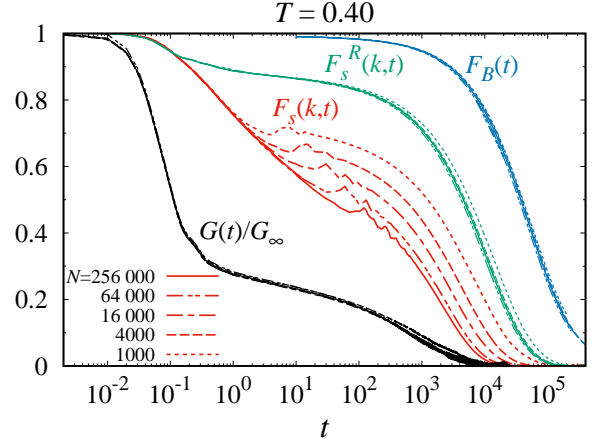


FIG. 1. Relaxation functions $F_s(k, t)$, $F_s^R(k, t)$, and $F_B(t)$ are plotted for system sizes $N = 256000$, 64000 , 16000 , 4000 , and 1000 at $T = 0.40$. The corresponding stress relaxation function $G(t)$ is also plotted (normalized with respect to the instantaneous shear modulus G_∞).

const. between the diffusivity D and the viscosity η . This relation holds in normal liquids at high temperatures, but is violated in the deeply supercooled regime [21, 31, 35–37]. In simulation studies of glass-forming liquids, because the microscopic structural relaxation time is expected to grow proportionally with the viscosity, the left-hand quantity $D\eta/T$ (the so-called SE ratio) is often replaced by the product of the diffusivity and the relaxation time $D\tau_\alpha$, and its T -dependence is usually examined. This assumption may break down in two dimensions because τ_α is robustly suppressed by the long-wavelength fluctuations. Thus, we calculate the temperature-dependence of the generalized SE ratio $D\tau$ to examine how the three relaxation times change with respect to the diffusivity D as the temperature decreases. We further compare $D\tau$ with the original SE ratio $D\eta/T$. This is done by explicitly calculating the shear viscosity η via the Green–Kubo formula $\eta = \int G(t) dt$ [21, 23], for which we require an error estimate because of the slow convergence of this integral [24].

In Fig. 2 (a)–(c), the original SE ratio $D\eta/T$ is shown for system sizes of $N = 1000$, 16000 , and 256000 as functions of the inverse temperature; the generalized SE ratios $D\tau_\alpha$, $D\tau_R$, and $D\tau_B$ are also shown. Although the diffusivity D has a logarithmic dependence on the system size N , the generalized SE ratios can be meaningfully compared across different values of N because of their similar temperature dependence [24]. Firstly, the standard SE ratio increases as the temperature decreases, as in 3D systems. However, $D\tau_\alpha$ exhibits system-size dependence and nonmonotonic temperature dependence and is clearly decorrelated from $D\eta/T$, which is consistent with the results of a previous study [21]. In contrast, $D\tau_R$ collapses to the standard SE ratio for all system sizes, showing that the neighbor-relative relaxation time τ_R grows in proportion to the viscosity, satisfying $\tau_R \sim \eta/T$ (see also Fig. 2(d)). This relation provides an alternative to $\tau_\alpha \sim \eta/T$ [35, 37–39], and thus

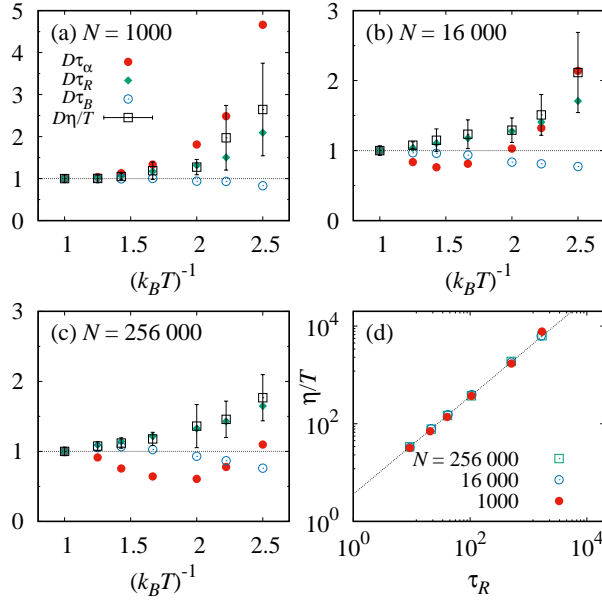


FIG. 2. (a)–(c) SE ratios for (a) $N = 1000$, (b) 16000, and (c) 256000 are shown as functions of the inverse temperature. Error bars indicate the standard deviation arising from the variation in η between independent runs. (d) η/T is plotted as a function of the neighbor-relative relaxation time τ_R for different N .

τ_R clearly takes the role of the microscopic structural relaxation time. We also find that the generalized SE ratio for bond relaxation is preserved, *i.e.*, $D \propto \tau_R^{-1}$, indicating that the bond relaxation function is a descriptor for the 2D diffusive motion in a similar manner to other 3D supercooled liquids [31, 39].

Thus far, we have seen that the diffusivity and viscosity are linked to time scales associated with local particle motion that is irrelevant to the long-wavelength fluctuations. However, this is not the end of our discussion, and we further investigate the hydrodynamic effects on the diffusivity by thoroughly examining the dependence on the system size. As shown in Fig. 3(a) for $T = 0.4$, the mean-squared displacements (MSDs) $\langle |\Delta \mathbf{r}(t)|^2 \rangle = (1/N) \langle \sum_{i=1}^N |\mathbf{r}_i(t + t_0) - \mathbf{r}_i(t_0)|^2 \rangle$ exhibit linear growth and remain dependent on the system size in the long-time limit. For temperatures $0.4 \leq T \leq 1.0$, we further estimate the diffusivity D by fitting $D = \langle |\Delta \mathbf{r}(t)|^2 \rangle / 4t$ in the long-time region $10 \leq \langle |\Delta \mathbf{r}(t)|^2 \rangle \leq 20$ for different system sizes. The result is shown as a function of the box length L in Fig. 3(b). The diffusivity D grows logarithmically with system size, even at low temperatures. This size dependence cannot arise from a simple superposition of elastic vibrational fluctuations (the so-called “Mermin–Wagner fluctuations” [9]), but should be attributed to a different origin.

As a statistical measure for the motion of individual particles, the velocity autocorrelation function (VACF) $Z(t) = (1/d) \langle \mathbf{v}(t) \cdot \mathbf{v}(0) \rangle$ [19] contains information regarding the delay in the viscoelastic responses of liquids. Importantly, VACF is related to the diffusivity via the Green–Kubo formula $D = \int_0^\infty Z(t) dt$, and should provide clues as to the system-size dependence. However, calculating the full resolution of VACF

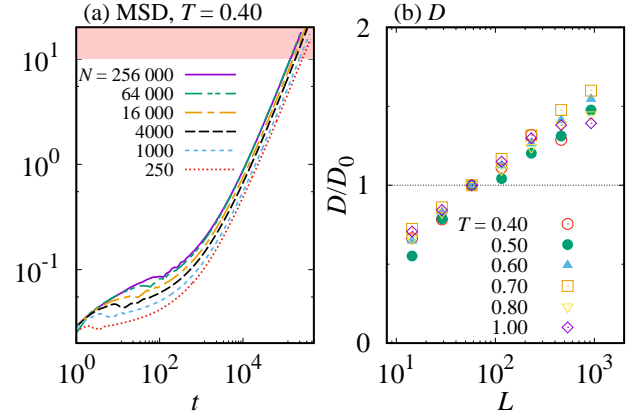


FIG. 3. (a) MSDs are plotted for system sizes $N = 256000, 64000, 16000, 4000, 1000$, and 250 at $T = 0.40$. Shaded region indicates the fitting region for evaluation of diffusivity. (b) Diffusivity D as a function of box length L . The corresponding particle number ranges over $250 \leq N \leq 1024000$. For each temperature, the data are normalized with respect to D_0 , the diffusivity at $N = 4000$.

for a glass-forming liquid is a difficult task, because random motions of the caged particles blur the slow process of diffusion. In a high-density 3D liquid at a moderately high temperature, the VACF exhibits a negative correlation in the intermediate time regions [40–42], which can be attributed to the velocity reversal caused by elastic vibrations of tagged particles [41]. Hence, for the present dense 2D liquid, we focus on high temperatures to demonstrate the crossover from transient elastic response to long-time hydrodynamic decay over a full time range. Figure 4(a) shows the VACF for different system sizes N at $T = 1.0$. Negative correlations exist for all N , indicating backward motion originating from elastic vibrations (see the plot for $N = 256000$ in the inset). However, VACF does not simply decay from negative values to zero, but becomes positive over a longer time range for sufficiently large system sizes, such as $N \geq 256000$. By examining a much larger system size ($N = 4096000$), the long-time limiting behavior is found to be consistent with the hydrodynamic t^{-1} tail that appears in normal 2D liquids [16–19, 43, 44]. Because the kinematic viscosity is large, *i.e.*, $\nu = \eta/(nm) \gg D$, the analytical expression can be simplified to $Z(t) = (k_B T / 8\pi\eta) t^{-1}$. Both the magnitude and power-law exponent of VACF coincide with this expression. Therefore, the system size dependence of diffusivity D is attributed to the purely hydrodynamic origin in the long-time limit where the transient elastic response vanishes.

Notably, the VACF itself exhibits system-size dependence at times before the t^{-1} power-law tail. For each N , the VACF exhibits a systematic decrease before becoming uncorrelated. In Fig. 4(b), we show the size dependence of the finite-time diffusivity

$$D'(t) = \int_0^t Z(t) dt \quad (3)$$

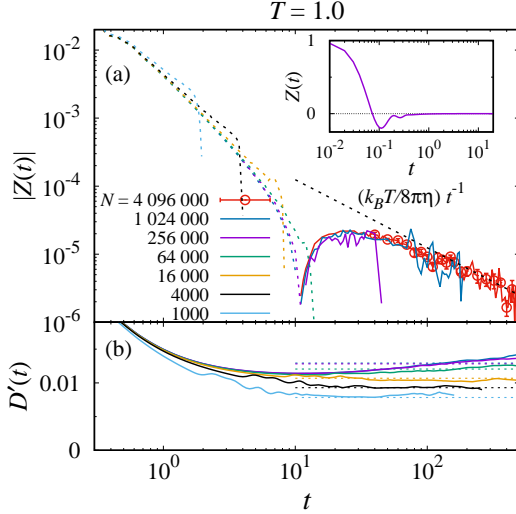


FIG. 4. (a) Absolute value of VACF $|Z(t)|$ for different system sizes at $T = 1.0$. The solid and dotted lines indicate that the corresponding VACFs assume positive and negative values, respectively. The data are only displayed over short time periods for small N , for ease of visibility. The straight line indicates the hydrodynamic long-time tail $Z(t) = (k_B T / 8\pi\eta)t^{-1}$. Inset: Semi-log plot of the raw value of VACF for $N = 256000$. (b) Time-dependent diffusivity, calculated by the Green-Kubo formula $D'(t) = \int_0^t Z(t) dt$ for different system sizes. Dotted lines indicate the diffusivity D evaluated from the MSD in Fig. 3(b).

in which the long-time limit yields the long-time diffusivity $D = \lim_{t \rightarrow \infty} D'(t)$. This finite-time diffusivity $D'(t)$ is in good agreement with the diffusivity D evaluated from MSD in the long-time limit. At the same time, it exhibits size dependence in an *earlier* time range, before converging to the long-time diffusivity D . Therefore, quite reasonably, the VACF $Z(t)$ itself is affected by the hidden hydrodynamic long-time tail, which has been difficult to find in simulations of 2D glass-forming liquids [21, 23, 36, 45].

The above results suggest that the origin of the logarithmic divergence of diffusivity is the t^{-1} long-time tail and that it should exist even at low temperature. The long-time tail $Z(t) = (k_B T / 8\pi\eta)t^{-1}$ no longer involves the diffusivity D in its expression and is free from the self-consistency problem leading to a faster than t^{-1} decay [18]. Therefore, the diffusivity simply diverges as

$$D \sim \frac{k_B T}{8\pi\eta} \ln\left(\frac{L}{\sigma_{11}}\right). \quad (4)$$

Hydrodynamic theories also predicts the t^{-1} tail in the shear stress autocorrelation function, which may cause logarithmic divergence of shear viscosity [16]. The shear stress autocorrelation functions is calculated for the same temperature but still such a power-law tail is not clear with the system size $N = 4096000$ [24].

It is worth noting that the analytic expression Eq. (4) brings about increase of SE ratio $D\eta/T \sim \ln L$ over all the temper-

ature ranges. This ratio increases by an order of magnitude if the system length L increases by five orders of magnitude. While a common expectation seems to be that the effect of long-time tail is marginal in 2D glass transitions [45], it is clear that the long-time tail also causes violation of SE relation, indicating that it may influence the 2D glass transition.

Finally, we address the relevance of our results to recent studies. A recent simulation study on the same 2D Kob-Andersen liquid reported that the mean-square of the neighbor-relative displacement (*i.e.*, cage-relative MSD) asymptotically approaches the normal MSD in the long-time limit [23]. Together with our observation of the finite size effects in the MSD, their result implies that the neighbor-relative displacement is also system-size dependent, finally approaching the linear behavior of the usual MSD and giving rise to the same diffusivity. However, the neighbor-relative relaxation time τ_R is short enough such that it remains virtually unaffected by the long-wavelength fluctuations. Therefore, our present results fully justify the usage of the equivalent cage-relative SISF in recent colloidal experiments [9, 10].

We note that our results rely on the use of the *NVE* ensemble to conserve the total momentum. Both the thermal vibrations and the hydrodynamic fluctuations at long wavelengths are suppressed by using the Brownian dynamics [8] or specialized Monte Carlo algorithms [46]. It has long been assumed that glassy dynamics are unaffected by the choice of ensembles, as in 3D liquids [47], but this is not the case in two dimensions for quantities that are affected by long-wavelength elastic and hydrodynamic fluctuations, including the standard SISF and the MSD.

In conclusion, the dynamics of a 2D glass-forming liquid are covered by hydrodynamic power-law correlations that lead to the logarithmic divergence of diffusivity, in addition to the recently revealed long-wavelength elastic fluctuations arising from the emerging rigidity of the liquid. Both the elastic and hydrodynamic fluctuations persists at long-wavelengths to produce a concerted effects on the transport properties. Moreover, it is found that the relaxation time defined from the relative displacement between neighbors (τ_R) grows in proportion to η/T as the temperature decreases, implying that local density fluctuations govern the drastic increase in viscosity. The combined elastic and hydrodynamic anomalies are expected to be relevant to both the existence of the 2D glass transition [46] and the dynamical features of 2D crystal melting, although further clarification is required in forthcoming studies.

Acknowledgements We thank Hajime Tanaka, Kunimasa Miyazaki, and Patrick A. Bonnaud for fruitful discussions. This work was supported by JSPS KAKENHI Grant Numbers JP18K13513 (H. S.), JP19K03767 (T. K.), and JP18H01188 (K. K.). H. S. was also financially supported by Building of Consortia for the Development of Human Resources in Science and Technology, Ministry of Education, Culture, Sports, and Technology (MEXT), Japan. The numerical calculations were performed on the Cray XC50-LC at the Institute for Materials Research, Tohoku University, Japan, the NEC

LX406Rh-2 at the Research Center of Computational Science, Okazaki Research Facilities, National Institutes of Natural Sciences, Japan, and the SGI ICE XA and HPE SGI 8600 at the Institute for Solid State Physics, University of Tokyo, Japan.

-
- [1] B. I. Halperin and David R. Nelson, “Theory of Two-Dimensional melting,” *Phys. Rev. Lett.* **41**, 121–124 (1978).
- [2] K. Zahn, R. Lenke, and G. Maret, “Two-Stage Melting of Paramagnetic Colloidal Crystals in Two Dimensions,” *Phys. Rev. Lett.* **82**, 2721–2724 (1999).
- [3] Y. Han, N. Y. Ha, A. M. Alsayed, and A. G. Yodh, “Melting of two-dimensional tunable-diameter colloidal crystals,” *Phys. Rev. E* **77**, 041406 (2008).
- [4] H. Shiba, A. Onuki, and T. Araki, “Structural and dynamical heterogeneities in two-dimensional melting,” *EPL* **86**, 66004 (2009).
- [5] S. C. Kapfer and W. Krauth, “Two-dimensional melting: From liquid-hexatic coexistence to continuous transitions,” *Phys. Rev. Lett.* **114**, 035702 (2015).
- [6] A. L. Thorneywork, J. L. Abbott, Dirk G. A. L. Aarts, and Roel P. A. Dullens, “Two-Dimensional Melting of Colloidal Hard Spheres,” *Phys. Rev. Lett.* **118**, 158001 (2017).
- [7] H. Shiba, Y. Yamada, T. Kawasaki, and K. Kim, “Unveiling Dimensionality Dependence of Glassy Dynamics: 2D Infinite Fluctuation Eclipses Inherent Structural Relaxation,” *Phys. Rev. Lett.* **117**, 245701 (2016).
- [8] E. Flenner and G. Szamel, “Fundamental differences between glassy dynamics in two and three dimensions,” *Nat. Commun.* **6**, 7392 (2015).
- [9] B. Illing, S. Fritsch, H. Kaiser, C. L. Klix, G. Maret, and P. Keim, “Mermin–Wagner fluctuations in 2D amorphous solids,” *Proc. Natl. Acad. Sci. U. S. A.* **114**, 1856–1861 (2017).
- [10] S. Vivek, C. P. Kelleher, P. M. Chaikin, and E. R. Weeks, “Long-wavelength fluctuations and the glass transition in two dimensions and three dimensions,” *Proc. Natl. Acad. Sci. U. S. A.* **114**, 1850–1855 (2017).
- [11] H. Mizuno, H. Shiba, and A. Ikeda, “Continuum limit of the vibrational properties of amorphous solids,” *Proc. Natl. Acad. Sci. U. S. A.* **114**, E9767–E9774 (2017).
- [12] F. H. Stillinger, “A Topographic View of Supercooled Liquids and Glass Formation,” *Science* **267**, 1935–1939 (1995).
- [13] M. D. Ediger, C. A. Angell, and Sidney R. Nagel, “Supercooled liquids and glasses,” *J. Phys. Chem.* **100**, 13200–13212 (1996).
- [14] M. M. Hurley and P. Harrowell, “Non-Gaussian behavior and the dynamical complexity of particle motion in a dense two-dimensional liquid,” *J. Chem. Phys.* **105**, 10521–10526 (1996).
- [15] W. Götze, *Complex Dynamics of Glass-Forming Liquids: A Mode-Coupling Theory* (Oxford University Press, Oxford, 2009).
- [16] M. H. Ernst, E. H. Hauge, and J. M. J. van Leeuwen, “Asymptotic Time Behavior of Correlation Functions,” *Phys. Rev. Lett.* **25**, 1254–1256 (1970).
- [17] B. J. Alder and T. E. Wainwright, “Decay of the velocity autocorrelation function,” *Phys. Rev. A* **1**, 18–21 (1970).
- [18] M. A. van der Hoef and D. Frenkel, “Evidence for faster-than- t^{-1} decay of the velocity autocorrelation function in a 2d fluid,” *Phys. Rev. Lett.* **66**, 1591–1594 (1991).
- [19] J. P. Hansen and I. R. McDonald, *Theory of Simple Liquids* (Academic Press, New York, 2006).
- [20] W. Kob and H. C. Andersen, “Testing mode-coupling theory for a supercooled binary Lennard-Jones mixture: The van Hove correlation function,” *Phys. Rev. E* **51**, 4626–4641 (1995).
- [21] S. Sengupta, S. Karmakar, C. Dasgupta, and S. Sastry, “Breakdown of the Stokes-Einstein relation in two, three and four dimensions,” *J. Chem. Phys.* **138**, 12A548 (2013).
- [22] E. Flenner and G. Szamel, “Dynamic heterogeneity in two-dimensional supercooled liquids: comparison of bond-breaking and bond-orientational correlations,” *J. Stat. Mech.* **2016**, 074008 (2016).
- [23] E. Flenner and G. Szamel, “Viscoelastic shear stress relaxation in two-dimensional glass forming liquids,” *Proc. Natl. Acad. Sci. U. S. A.* **116**, 2015–2020 (2019).
- [24] See Supplemental Material [URL will be inserted by publisher] for the following details: simulation settings, interpretation of the plateau height of the SISF, definitions of the relaxation times, the stress relaxation function and evaluation procedure of viscosity, and temperature dependence of diffusivity.
- [25] B. Zhang and X. Cheng, “Long-wavelength fluctuations and static correlations in quasi-2d colloidal suspensions,” *Soft Matter* **15**, 4087–4097 (2019).
- [26] G. Pastore, B. Bernu, J. P. Hansen, and Y. Hiwatari, “Soft-sphere model for the glass transition in binary alloys. II. Relaxation of the incoherent density-density correlation functions,” *Phys. Rev. A* **38**, 454–462 (1988).
- [27] H. Tong and H. Tanaka, “Revealing Hidden Structural Order Controlling Both Fast and Slow Glassy Dynamics in Supercooled Liquids,” *Phys. Rev. X* **8**, 011041 (2018).
- [28] Y.-W. Li, C. K. Mishra, Z.-Y. Sun, K. Zhao, T. G. Mason, R. Ganapathy, and M. Pica Ciamarra, “Long-wavelength fluctuations and anomalous dynamics in 2-dimensional liquids,” *Proc. Natl. Acad. Sci. U. S. A.* **116**, 22977–22982 (2019).
- [29] R. Yamamoto and A. Onuki, “Dynamics of Highly Supercooled Liquids: Heterogeneity, rheology, and diffusion,” *Phys. Rev. E* **58**, 3515–3529 (1998).
- [30] H. Shiba, T. Kawasaki, and A. Onuki, “Relationship between bond-breakage correlations and four-point correlations in heterogeneous glassy dynamics: Configuration changes and vibration modes,” *Phys. Rev. E* **86**, 041504 (2012).
- [31] T. Kawasaki and A. Onuki, “Slow relaxations and stringlike jump motions in fragile glass-forming liquids: Breakdown of the Stokes-Einstein relation,” *Phys. Rev. E* **87**, 012312 (2013).
- [32] S. Mazoyer, F. Ebert, G. Maret, and P. Keim, “Dynamics of particles and cages in an experimental 2D glass former,” *EPL* **88**, 66004 (2009).
- [33] V. M. Bedanov, G. V. Gadiyak, and Yu E. Lozovik, “On a modified Lindemann-like criterion for 2D melting,” *Phys. Lett. A* **109**, 289–291 (1985).
- [34] K. Zahn and G. Maret, “Dynamic criteria for melting in two dimensions,” *Phys. Rev. Lett.* **85**, 3656–3659 (2000).
- [35] G. Tarjus and D. Kivelson, “Breakdown of the Stokes-Einstein relation in supercooled liquids,” *J. Chem. Phys.* **103**, 3071–3073 (1995).
- [36] B. Liu, J. Goree, and O. S. Vaulina, “Test of the Stokes-Einstein relation in a two-dimensional yukawa liquid,” *Phys. Rev. Lett.* **96**, 015005 (2006).
- [37] Z. Shi, P. G. Debenedetti, and F. H. Stillinger, “Relaxation processes in liquids: Variations on a theme by Stokes and Einstein,” *J. Chem. Phys.* **138**, 12A526 (2013).
- [38] R. Yamamoto and A. Onuki, “Heterogeneous Diffusion in Highly Supercooled Liquids,” *Phys. Rev. Lett.* **81**, 4915–4918 (1998).

- [39] T. Kawasaki and K. Kim, “Identifying time scales for violation/preservation of Stokes-Einstein relation in supercooled water,” *Sci. Adv.* **3**, e1700399 (2017).
- [40] B. J. Alder, D. M. Gass, and T. E. Wainwright, “Studies in molecular dynamics. viii. the transport coefficients for a hard-sphere fluid,” *J. Chem. Phys.* **53**, 3813–3826 (1970).
- [41] Stephen R. Williams, G. Bryant, I. K. Snook, and W. van Meegen, “Velocity autocorrelation functions of hard-sphere fluids: Long-time tails upon undercooling,” *Phys. Rev. Lett.* **96**, 087801 (2006).
- [42] H. L. Peng, H. R. Schober, and Th. Voigtmann, “Velocity autocorrelation function in supercooled liquids: Long-time tails and anomalous shear-wave propagation,” *Phys. Rev. E* **94**, 060601(R) (2016).
- [43] M. Isobe, “Long-time tail of the velocity autocorrelation function in a two-dimensional moderately dense hard-disk fluid,” *Phys. Rev. E* **77**, 021201 (2008).
- [44] B. Choi, K. H. Han, C. Kim, P. Talkner, A. Kidera, and E. K. Lee, “Nature of self-diffusion in two-dimensional fluids,” *New J. Phys.* **19**, 123038 (2017).
- [45] D. N. Perera and P. Harrowell, “Origin of the difference in the temperature dependences of diffusion and structural relaxation in a supercooled liquid,” *Phys. Rev. Lett.* **81**, 120–123 (1998).
- [46] L. Berthier, P. Charbonneau, A. Ninarello, M. Ozawa, and S. Yaida, “Zero-temperature glass transition in two dimensions,” *Nat. Commun.* **10**, 1508 (2019).
- [47] T. Gleim, W. Kob, and K. Binder, “How Does the Relaxation of a Supercooled Liquid Depend on Its Microscopic Dynamics?” *Phys. Rev. Lett.* **81**, 4404–4407 (1998).

Supplemental Material for “Local Density Fluctuation Governs the Divergence of Viscosity Underlying Elastic and Hydrodynamic Anomalies in a 2D Glass-Forming Liquid”

Hayato Shiba,¹ Takeshi Kawasaki,² and Kang Kim³

¹*Institute for Materials Research, Tohoku University, Sendai 980-8577, Japan*

²*Department of Physics, Nagoya University, Nagoya 464-8602, Japan*

³*Division of Chemical Engineering, Graduate School of Engineering Science, Osaka University, Osaka 560-8531, Japan*

I. SIMULATION SETTINGS AND MODELS

Simulations were performed for a 2D variant of Kob-Andersen binary Lennard-Jones mixtures in which the composition was 65:35 [S1–S5]. The pairwise potential was computed as a function of the interparticle distance r :

$$v_{\alpha\beta}(r) = 4\epsilon_{\alpha\beta} \left[\left(\frac{\sigma_{\alpha\beta}}{r} \right)^{12} - \left(\frac{\sigma_{\alpha\beta}}{r} \right)^6 \right] \quad (\text{S1})$$

and was truncated and shifted at $r = 2.5\sigma_{\alpha\beta}$. The parameters $\epsilon_{\alpha\beta}$ and $\sigma_{\alpha\beta}$ were set to standard values for arbitrary combinations of particle species $\{\alpha, \beta\} \in \{1, 2\}$ [S6]. The number density was fixed at $n = N/L^2 = 1.2$, where N and L denote the total particle number and the box length, respectively. Hereafter, the length, energy, and time are presented in units reduced by σ_{11} , ϵ_{11}/k_B , and $\sigma_{11}(m/\epsilon_{11})^{1/2}$, respectively, and the Boltzmann constant k_B is assumed to be unity. A liquid at a high temperature ($T = 2.5$) was rapidly cooled to target temperatures in the range $0.4 \leq T \leq 1.0$. The mixture was annealed for a sufficiently long time (4×10^9 time steps for the minimum temperature $T = 0.4$) in the presence of a Langevin heat bath. Subsequently, production runs were performed. In this step, we performed Newtonian (NVE) dynamics simulations to avoid the damping of long-wavelength fluctuations. The simulations were performed for system sizes $250 \leq N \leq 256\,000$ and temperatures $T = 0.4, 0.45, 0.5, 0.6, 0.7, 0.8$, and 1.0 , with a time step of 10^{-3} . The results were averaged over eight independent runs for each N and T , except for $T = 0.4$, where only four runs were averaged. For $N = 1\,024\,000$ and $4\,096\,000$, additional simulations (four runs for each) were performed for $0.45 \leq T \leq 1.0$ and $T = 1.0$, respectively.

II. PLATEAU HEIGHT OF THE SELF-INTERMEDIATE SCATTERING FUNCTION

As a standard relaxation function that is used for characterizing the glassy relaxation, the self-intermediate scattering function (SISF) $F_s(k, t)$, with the wavevector $k = 2\pi/\sigma_{11}$, was calculated (see Fig. 1 of the main text). If a plateau appears in the SISF, its height corresponds to the so-called Debye-Waller factor [S7]

$$f_p = \exp\left(-\frac{k^2 \delta^2}{d}\right), \quad (\text{S2})$$

which indicates the strength of the thermal vibrations of a single particle. Herein, δ^2 and d represent the mean-squared thermal displacement (MSTD) and spatial dimensionality, respectively. Owing to the Gaussian nature of the thermal fluctuation, MSTD is half its squared amplitude A^2 , that is, $A^2 = 2\delta^2$. In a two-dimensional (2D) glass-forming liquid, the short-time dynamics are dominated by the solid-like elastic response during supercooling. The MSTD in the plateau region is given by [S8]

$$\delta^2 \simeq \frac{k_B T}{2\pi m n} \left(\frac{1}{c_L^2} + \frac{1}{c_T^2} \right) \ln\left(\frac{L}{\sigma_{11}}\right). \quad (\text{S3})$$

This is a consequence of the Debye asymptote giving rise to an abundance of phonon densities of state at low frequencies (*i.e.*, at long wavelengths).

For the present 2D Kob-Andersen binary mixture, the longitudinal (c_L) and translational (c_T) sound velocities are estimated to be $c_L = 10.24$ and $c_T = 3.68$. In Fig. S1, the system-size dependence of the squared vibration amplitude $A^2 = 2\delta^2$ is evaluated from the plateau height of SISF. Its increase with system size coincides with Eq. (S3), which clearly accounts for the origin of the size dependence of SISF.

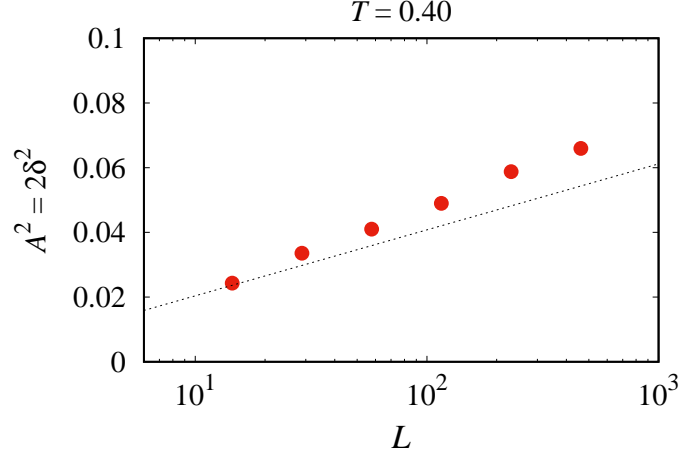


FIG. S1. Squared vibration amplitude $A_p^2 = 2\delta^2$, evaluated from the plateau height of SISF, as a function of the linear box length L . The broken line is an estimation from the phonon density of states in Eq. (S3).

III. DEFINITIONS OF RELAXATION TIMES

In addition to the SISF and the neighbor-relative SISF, we employ the bond relaxation function [S3, S8–S11], which characterizes changes in the number of neighbor particles. We first count the number of neighbor pairs at the initial time $N_B(t_0)$ satisfying

$$r_{ij}(t_0) = |\mathbf{r}_i(t_0) - \mathbf{r}_j(t_0)| < 1.2\sigma_{\alpha\beta}, \quad (\text{S4})$$

where $r_{ij}(t_0)$ is the distance between particles i and j at time t_0 . At a later time $t + t_0$, we count the number of pairs of particles $N_B(t_0 + t; t_0)$ that have become separated:

$$r_{ij}(t_0 + t) = |\mathbf{r}_i(t_0 + t) - \mathbf{r}_j(t_0 + t)| > 1.5\sigma_{\alpha\beta}. \quad (\text{S5})$$

Using these numbers, the bond relaxation function can be defined as

$$F_B(t) = 1 - \frac{N_B(t_0 + t; t_0)}{N_B(t_0)} \quad (\text{S6})$$

Based on the SISF, neighbor-relative SISF, and the bond relaxation function, we evaluated the relaxation times using the following procedures. First, the α -relaxation time τ_α was defined as the decay time of standard SISF $F_s(k, t)$. For the present 2D liquid, the decay in the SISF becomes faster as the system size becomes larger, thus deviating from the stretched exponential form. Therefore, we employ the criterion

$$F_s(k, \tau_\alpha) = 0.1 \quad (\text{S7})$$

for the determination of the α -relaxation time τ_α . The results in the main text do not change appreciably if $F_s(k, \tau_\alpha) = 1/e$ is employed, as in a previous study [S4]. For the neighbor-relative SISF $F_s^R(k, t)$, however, the relaxation behavior is well approximated by a double stretched exponential function [S1]

$$F_s^R(k, t) = (1 - f_c) \exp\left(-\frac{t}{\tau_s}\right) + f_c \exp\left[-\left(\frac{t}{\tau_R}\right)^\gamma\right], \quad (\text{S8})$$

where τ_s , τ_R , and γ are fitting parameters. This yields a proper evaluation of the neighbor-relative relaxation time τ_R . By fitting the temperature dependence of τ_R to the VogelFulcher-Tamman form $\tau_R = B \exp(A/(T - T_F))$, with B , A , and T_F as the fitting parameters, the glass transition temperature T_F can be estimated to be 0.201(2).

The bond relaxation time τ_B [S9, S10] is evaluated by the usual single stretched exponential fit of the bond relaxation function $F_B(t)$:

$$F_B(t) = \exp\left[-\left(\frac{t}{\tau_B}\right)^\beta\right], \quad (\text{S9})$$

where τ_B and β are fitting parameters.

IV. STRESS RELAXATION FUNCTION AND EVALUATION PROCEDURE OF VISCOSITY

In evaluating the viscosity η using the Green-Kubo formula

$$\eta = \int G(t) dt, \quad G(t) = \frac{V}{k_B T} \langle \sigma_{xy}(t) \sigma_{xy}(0) \rangle, \quad (\text{S10})$$

the stress relaxation function $G(t)$ is calculated from the trajectory of each independent run and is numerically integrated over time. We set the upper limit of the integration to the time at which $G(t)$ becomes less than zero for the first time (in each run). We averaged the resulting values of η over eight (or four for $T = 0.4$) independent simulation runs, and estimated the standard deviation.

In Fig. S2, a logarithmic plot of the stress relaxation functions $G(t)$ is given for various temperatures. The system size is $N = 4\,096\,000$ for $T = 1.0$, and $N = 256\,000$ for other temperatures. We find a formation of plateau, but as noted in Ref. S4, it cannot be well fitted by the stretched exponential function for $T \geq 0.7$. In a 2D liquid, the so-called hydrodynamic long-time tail should also appear in $G(t)$. At $T = 1.0$, there is a symptom of the power-law tail, but the error is still too large to conclude its existence. Therefore, it is left for future large-scale simulations.

However, the variance of η mainly arises from the plateau-like regions of $G(t)$, rather than from the longer-time relaxation close to the cutoff where such behavior might exist. The viscosity (in terms of the Green-Kubo formula) does not vary significantly with the long-time tail of $G(t)$, even if it exists, because the majority of the contribution and statistical errors arise from the intermediate time window.

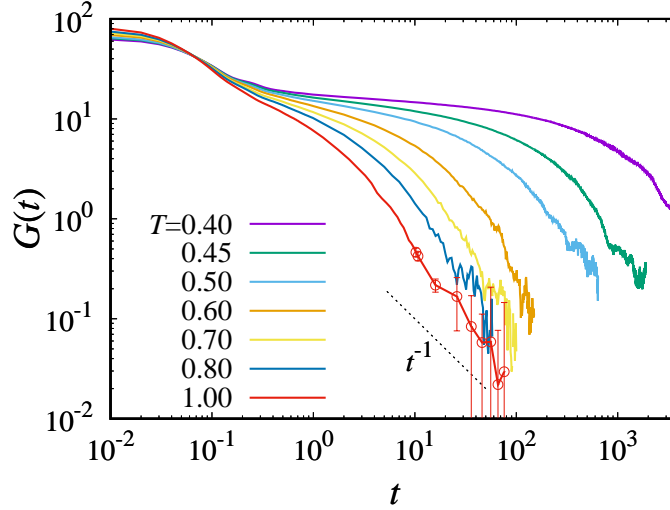


FIG. S2. Stress relaxation function $G(t)$ for various temperatures. The system size is $N = 256\,000$, except for $N = 4\,096\,000$ at $T = 1.0$. The errors for $T = 1.0$ are evaluated from four independent simulations.

V. TEMPERATURE DEPENDENCE OF THE DIFFUSIVITY

In the 2D glass-forming liquid under consideration, diffusivity D is found to be influenced by long-wavelength hydrodynamic fluctuations that are dependent on the system size, contrary to the behavior in higher dimensions. Although this situation is beyond what is assumed in the Stokes-Einstein (SE) relation, the temperature dependence of diffusivity itself remains similar at different system sizes as the temperature decreases, as shown in Fig. S3. Therefore, the SE ratios ($D\eta/T$ or $D\tau$) can still be employed to examine the relationship between the diffusivity and the viscosity.

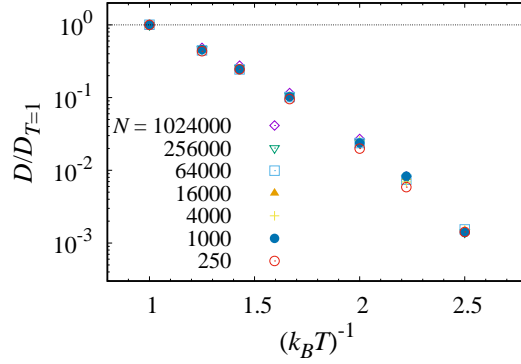


FIG. S3. Diffusivity D evaluated from the MSDs as functions of the inverse temperature for system sizes $250 \leq N \leq 1\,024\,000$.

-
- [S1] S. Sengupta, S. Karmakar, C. Dasgupta, and S. Sastry, J. Chem. Phys. **138**, 12A548 (2013).
 - [S2] E. Flenner and G. Szamel, Nat. Commun. **6**, 7392 (2015).
 - [S3] E. Flenner and G. Szamel, J. Stat. Mech. **2016**, 074008 (2016).
 - [S4] E. Flenner and G. Szamel, Proc. Natl. Acad. Sci. U. S. A. **116**, 2015 (2019).
 - [S5] Y.-W. Li, C. K. Mishra, Z.-Y. Sun, K. Zhao, T. G. Mason, R. Ganapathy, and M. Pica Ciamarra, Proc. Natl. Acad. Sci. U. S. A. **116**, 22977 (2019).
 - [S6] W. Kob and H. C. Andersen, Phys. Rev. E **51**, 4626 (1995).
 - [S7] G. Pastore, B. Bernu, J. P. Hansen, and Y. Hiwatari, Phys. Rev. A **38**, 454 (1988).
 - [S8] H. Shiba, Y. Yamada, T. Kawasaki, and K. Kim, Phys. Rev. Lett. **117**, 245701 (2016).
 - [S9] R. Yamamoto and A. Onuki, Phys. Rev. E **58**, 3515 (1998).
 - [S10] H. Shiba, T. Kawasaki, and A. Onuki, Phys. Rev. E **86**, 041504 (2012).
 - [S11] T. Kawasaki and A. Onuki, Phys. Rev. E **87**, 012312 (2013).